DALTON
FULL PAPER

The use of spectroelectrochemistry to probe the redox-activated ligand-exchange reactions of the complexes *trans*-$[NBu_4][RuX_4(CNXyl)_2]$ (X = Cl or Br, Xyl = 2,6-dimethylphenyl)

Joseph P. al Dulaimi,[a] **Alan M. Bond,***[b] **Robin J. H. Clark,***[a] **Nicholas C. Harden**[b] **and David G. Humphrey** *†[a,b]

[a] *Christopher Ingold Laboratories, University College London, 20 Gordon Street, London, UK WC1H 0AJ. E-mail: r.j.h.clark@ucl.ac.uk*
[b] *School of Chemistry, Monash University, PO Box 23, Victoria 3800, Australia. E-mail: Alan.Bond@sci.monash.edu.au*

Received 18th September 2001, Accepted 22nd March 2002
First published as an Advance Article on the web 15th May 2002

The previously unreported complexes *trans*-$[NBu_4][RuX_4(CNXyl)_2]$ (X = Cl or Br, Xyl = 2,6-dimethylphenyl) have been prepared by treating $[NBu_4]_2[RuX_6]$ with the isocyanide ligand CNXyl in dichloromethane–ethanol and characterised by IR and UV-Vis spectroscopy, fast-atom-bombardment mass spectrometry, and elemental analysis (C, H, N and X). Their solution redox chemistry has been investigated using electrochemical and *in situ* spectroelectrochemical techniques. At low temperatures each complex undergoes a one-electron reduction to *trans*-$[RuX_4(CNXyl)_2]^{2-}$ (X = Cl or Br). At ambient temperature the same complexes undergo reduction in the presence of acetonitrile to afford *mer*,*trans*-$[RuX_3(CNXyl)_2(NCMe)]^-$, which can be oxidised reversibly to *mer*,*trans*-$[RuX_3(CNXyl)_2(NCMe)]$ (X = Cl or Br). Simulation of the cyclic voltammograms of $[NBu_4][RuX_4(CNR)_2]$ (X = Cl or Br, R = Xyl or Bu^t) in acetonitrile has enabled the rate constants for the formation of *mer*,*trans*-$[RuX_3(CNR)_2(NCMe)]^-$ to be evaluated. The rate constants were found to vary in the order X = Cl, R = Xyl < X = Br, R = Xyl < X = Cl, R = Bu^t < X = Br, R = Bu^t. The oxidation of *trans*-$[RuX_4(CNXyl)_2]^-$ (X = Cl or Br) in acetonitrile is accompanied by the reductive elimination of $X^\bullet$. The number of product(s) formed is dependent upon the identity of the halide. For X = Cl oxidation ultimately leads to the formation of several species, which include *mer*,*trans*-$[RuCl_3(CNXyl)_2(NCMe)]$ and *trans*,*trans*,*trans*-$[RuCl_2(CNXyl)_2(NCMe)_2]^+$, whereas for X = Br oxidation only produces *mer*,*trans*-$[RuBr_3(CNXyl)_2(NCMe)]$. All of the redox products have been characterised *in situ* by IR and UV-Vis spectroscopy in as many oxidation states as possible.

Introduction

Recently the redox chemistry of *trans*-$[RuX_4(CNBu^t)_2]^-$ (X = Cl or Br), was described in considerable detail.[1,2] Electrochemical and spectroelectrochemical studies indicate that these ions undergo one-electron reduction to yield transient species which are presumed to be *trans*-$[RuX_4(CNBu^t)_2]^{2-}$. The latter readily undergo substitution reactions with a neutral donor ligand (L) to form species such as *mer*,*trans*-$[RuX_3(CNBu^t)_2L]^-$ (L = NCMe or py) or *trans*,*trans*,*trans*-$[RuX_2(CNBu^t)_2L_2]$ (L = PPh_3 or $CNBu^t$). Although the initial reduction products are stable at low temperature on the timescale of a voltammetric experiment, their lifetimes are found to be too short for characterisation by *in situ* spectroelectrochemical techniques.

As an extension to this work, the redox chemistry of the related 2,6-dimethylphenyl isocyanide complexes, *trans*-$[NBu_4][RuX_4(CNXyl)_2]$ (X = Cl or Br) has been investigated. This was undertaken in an attempt to characterise the initial products of reduction of *trans*-$[RuX_4(CNR)_2]^-$. The aryl isocyanide ligand, CNXyl, is considered to be a poorer σ-donor and a better π-acceptor than $CNBu^t$.[3] The increased capacity of CNXyl to π back-bond with Ru(II) was expected to provide additional stabilisation of the reduced species, and therefore permit their characterisation by *in situ* spectroelectrochemical techniques. The results of electrochemical and spectroelectrochemical studies of previously unreported *trans*-$[NBu_4][RuX_4(CNXyl)_2]$ (X = Cl or Br) are discussed herein. The voltammetry of the CNXyl and $CNBu^t$ complexes has also been simulated to determine the rate constants for the substitution of halide by acetonitrile in the formation of *mer*,*trans*-$[RuX_3(CNR)_2(NCMe)]^-$ (X = Cl or Br, R = Xyl or Bu^t).

Experimental

Synthesis

$RuCl_3\cdot xH_2O$, *x* assumed to be 3 (Johnson Matthey p.l.c.), CNXyl and $CNBu^t$ (both Fluka Chemicals Ltd) were used as received. *Trans*-$[NBu_4][RuX_4(CNBu^t)_2]$ (X = Cl or Br) was prepared as described previously,[4] and *trans*-$[NBu_4][RuX_4(CNXyl)_2]$ (X = Cl or Br) by a modification of this procedure.[5] The complexes were characterised by UV-Vis, IR and far-IR spectroscopy, fast-atom-bombardment mass spectrometry, and elemental analysis (C, H, N and X).

Potassium hexachlororuthenate(IV). $K_2[RuCl_6]$ was prepared by a method similar to that described by Griffith *et al.*[6] $RuCl_3\cdot xH_2O$ (0.20 g, 0.77 mmol) was added to conc. HCl (9.0 cm^3) and the mixture held under reflux for 1 h. Insoluble material was filtered off and the filtrate cooled in an ice-bath. Cl_2 was bubbled through the cooled solution for 10 min, the ice removed, and Cl_2 bubbled through the mixture for a further 15 min. An excess of finely ground KCl (0.15 g, 2.01 mmol) was then added and the mixture stirred at room temperature for

---

† Present address: CSIRO Forestry and Forest Products, Private Bag 10, Clayton South MDC, Victoria 3169, Australia. E-mail: David.Humphrey@ffp.csiro.au

DOI: 10.1039/b108474g

30 min. Cooling the solution resulted in the formation of the black product, which was collected by vacuum filtration, washed with a little ice-cold water and then with diethyl ether (0.22 g, 73%).

Potassium hexabromoruthenate(IV). Bluish-black $K_2[RuBr_6]$ (0.38 g, 75%) was prepared by a procedure similar to that used for $K_2[RuCl_6]$, using $RuCl_3{\cdot}xH_2O$ (0.20 g, 0.77 mmol), conc. HBr (12.0 cm^3), Br_2 (7.0 cm^3) and KBr (0.20 g, 1.68 mmol).

Tetrabutylammonium hexachlororuthenate(IV). $K_2[RuCl_6]$ (0.20 g, 0.51 mmol) was dissolved in 2 mol dm^{-3} HCl (15.0 cm^3) and $[NBu_4]Cl$ (0.57 g, 2.05 mmol) added, resulting in the formation of a brown solid. After stirring the mixture for 30 min at room temperature the brown product was filtered off under vacuum, washed with a little ice-cold water and then with diethyl ether. The addition of a further quantity of $[NBu_4]Cl$ (0.57 g, 2.05 mmol) to the filtrate yielded a second crop of $[NBu_4]_2[RuCl_6]$. The crude product was recrystallised from dichloromethane–diethyl ether and dried *in vacuo.* (0.36 g, 88%).

Tetrabutylammonium hexabromoruthenate(IV). $[NBu_4]_2$-$[RuBr_6]$ was prepared using the method described by Preetz and Allwörden.[7] $K_2[RuBr_6]$ (0.20 g, 0.30 mmol) was dissolved in ice-cold 3.0 mol dm^{-3} HBr (60.0 cm^3). This solution was extracted with dichloromethane (3 × 25.0 cm^3) containing $[NBu_4]Br$ (0.20 g, 0.62 mmol). The organic phase was washed with 2 mol dm^{-3} H_2SO_4 and dried over anhydrous Na_2SO_4. After filtration, the volume of the solution was reduced to approximately 20 cm^3 and n-hexane–diethyl ether (1 : 3, v : v, 20 cm^3) added, whereupon dark-blue plates formed upon cooling to 243 K. The product was collected by vacuum filtration, washed with diethyl ether and dried *in vacuo.* (0.21 g, 65%).

Tetrabutylammonium *trans*-tetrachlorobis(2,6-dimethylphenyl isocyanide)ruthenate(III). The isocyanide CNXyl (0.49 g, 3.75 mmol) was added to a stirred solution of $[NBu_4]_2[RuCl_6]$ (0.20 g, 0.25 mmol) in dichloromethane–ethanol (20 : 1, v : v, 30 cm^3). The resulting solution was heated to reflux under a nitrogen atmosphere until it turned from reddish-brown to yellow (48 h). The reaction mixture was reduced to dryness and the residue dissolved in dichloromethane. Diethyl ether was added to precipitate the crude product, which was redissolved in dichloromethane and filtered under gravity to remove an insoluble by-product. The crude product was recrystallised from dichloromethane–diethyl ether to give a yellow powder (0.15 g, 80%). Found: C, 54.6; H, 7.4; Cl, 19.1; N, 5.6. $C_{34}H_{54}Cl_4N_3Ru$ requires C, 54.61; H, 7.28; Cl, 18.97; N, 5.62%.

Tetrabutylammonium *trans*-tetrabromobis(2,6-dimethylphenyl isocyanide)ruthenate(III). Purple $[NBu_4][RuBr_4(CNXyl)_2]$ (0.12 g, 69%) was prepared from $[NBu_4]_2[RuBr_6]$ (0.20 g, 0.30 mmol) and CNXyl (0.49 g, 3.75 mmol) by a similar procedure to that described for the chloro-analogue. Found: C, 43.5; H, 5.7; Br; 35.4; N, 4.3. $C_{34}H_{54}Br_4N_3Ru$ requires C, 44.12; H, 5.88; Br, 34.53; N, 4.54%.

Electrochemical measurements

Electrochemical measurements: The majority of voltammetric experiments were performed using a single compartment cell which supported a platinum-bead working electrode, a platinum-coil auxiliary electrode and a Ag–AgCl reference electrode (0.45 mol dm^{-3} $[NBu_4][PF_6]$ and 0.05 mol dm^{-3} $[NBu_4]Cl$), against which the ferrocenium–ferrocene ($Fc^{+/0}$) couple was measured to be +0.55 V. Instrumentation consisted of a PAR 174A polarographic analyser and a PAR 175 waveform generator, used in conjunction with a Bryans 60000 series X–Y/t recorder. All voltammetric data were uncorrected for IR (ohmic) drop. Bulk electrolyses were carried out in a two-compartment cell, with a platinum-basket working electrode and Ag–AgCl reference electrode separated from the platinum auxiliary electrode by a double-fritted salt bridge. Solvents and electrolytes were dried and prepared as described previously.[8] Voltammograms used for comparison with simulation were recorded using a BAS 100B electrochemical analyser, platinum-disc working electrode (radius = 1 mm), a platinum-wire auxiliary electrode and a Ag–Ag^+ reference electrode (0.01 mol dm^{-3} $AgNO_3$, 0.1 mol dm^{-3} $[NBu_4][PF_6]$ in acetonitrile–dichloromethane). The diffusion coefficients (D) were calculated from steady-state voltammograms recorded with a platinum-microdisc working electrode (radius = 5 μm), using the equation $I_L = 4nFrCD$, where I_L = limiting current, n = number of electrons, F = the Faraday constant, r = electrode radius and C = concentration.[9] The kinetic parameters were obtained by simulation using DigiSim® version 3.03.[10]

Spectroelectrochemical measurements

In situ IR spectroelectrochemical experiments were performed as described previously using an infrared reflection-absorption spectroscopic (IRRAS) cell,[11,12] mounted on a modified Specac specular reflectance attachment (PN 19.170), in the sample compartment of a Nicolet 750 or a Bruker IFS 55 FTIR spectrometer. The electrode arrangement consisted of a polished platinum-disk working electrode (radius = 2.5 mm), a platinum-basket auxiliary electrode, and a silver-wire pseudo-reference electrode. UV-Vis spectroelectrochemical experiments were performed using an optically transparent thin-layer electrolysis (OTTLE) cell,[2] mounted in the sample compartment of a Perkin-Elmer Lambda 16 UV-Vis or Cary 5 UV-Vis-NIR spectrophotometer. For those complexes that were electrogenerated quantitatively and characterised *in situ* by UV-Vis spectroscopy, molar absorption coefficients (ε) were calculated from the ε values of the starting complexes *trans*-$[NBu_4]$-$[RuX_4(CNXyl)_2]$ (X = Cl or Br), which had been previously measured by conventional means.

Results and discussion

Synthesis and characterisation of *trans*-$[NBu_4][RuX_4(CNXyl)_2]$ (X = Cl or Br)

Several routes were investigated to prepare organo-soluble salts of $[RuX_4(CNXyl)_2]^-$. The method previously described for the synthesis of $[NBu_4][RuCl_4(CNBu^t)_2]$ involved boiling a dichloromethane solution of $[NBu_4]_2[RuCl_6]$ with a large excess of the isocyanide ligand $CNBu^t$ until the solution changed colour from red–brown to yellow;[4] in this work the reaction took approximately 1 week. Repeating this reaction with CNXyl gave the desired product, $[NBu_4][RuCl_4(CNXyl)_2]$, in *ca.* 65% yield. Both the reaction time and the quantity of isocyanide ligand required to form the product were reduced significantly upon addition of 5% absolute ethanol (v : v) to the reagent mixture. This procedure did, however, lead to the formation of unknown Ru(II) species which proved difficult to separate from the desired product.

The analogous bromide complex was initially prepared by the method reported for $[NBu_4][RuBr_4(CNBu^t)_2]$;[4] the method involved stirring a dichloromethane solution of $K_3[Ru_2Br_9]$ with the free isocyanide ligand and $[NBu_4]Br$ for >1 week. However the product, $[NBu_4][RuBr_4(CNXyl)_2]$, was found to crystallise with $[NBu_4]Br$ which was surprisingly difficult to separate from the product by fractional recrystallisation. Other salts of $[RuBr_4(CNXyl)_2]^-$ (and $[RuBr_4(CNBu^t)_2]^-$) could be prepared *via* the same route using different phase-transfer reagents, *e.g.* $[PPh_4]Br$ or $[PPh_3Bz]Br$, but these were also difficult to obtain free from contamination by bromide salts. Use of $[PF_6]^-$ or $[BF_4]^-$ salts of these cations produced only very

Table 1 FAB mass spectral data on *trans*-$[NBu_4][RuX_4(CNR)_2]$ (X = Cl or Br, R = Xyl or Bu^t)

Complex[a]	*m*/*z* (% base peak, assignment)[b]
$[NBu_4][RuCl_4(CNBu^t)_2]$	409 (45, M^-), 325 (56, M^- − $CNBu^t$), 288 (56, M^- − $CNBu^t$ − Cl), 243 (95, M^- − $2CNBu^t$), 208 (100, M^- − $2CNBu^t$ − Cl)
$[NBu_4][RuBr_4(CNBu^t)_2]$	587 (24, M^-), 504 (50, M^- − $CNBu^t$), 421 (100, M^- − $2CNBu^t$), 342 (49, M^- − $2CNBu^t$ − Br), 183 (45, M^- − $2CNBu^t$ − 3Br)
$[NBu_4][RuCl_4(CNXyl)_2]$	504 (18, M^-), 469 (54, M^- − Cl), 433 (24, M^- − 2Cl), 375 (50, M^- − CNXyl), 342 (37, M^- − CNXyl − Cl), 307 (42, M^- − CNXyl − 2Cl)
$[NBu_4][RuBr_4(CNXyl)_2]$	683 (45, M^-), 605 (54, M^- − Br), 552 (100, M^- − CNXyl), 471 (24, M^- − CNXyl − Br), 423 (50, M^- − 2CNXyl), 343 (63, M^- − 2CNXyl − Br), 319 (29, M^- − CNXyl − 3Br), 232 (52, M^- − CNXyl − 4Br)

[a] *trans* isomers. [b] Negative-ion FAB mass spectra recorded in 3-nitrobenzylalcohol matrix (*m*/*z* = 153).

Table 2 Electrode potentials of *trans*-$[NBu_4][RuX_4(CNR)_2]$ (X = Cl or Br, R = Xyl or Bu^t) and *mer,trans*-$[RuX_3(CNXyl)_2(NCMe)]$ (X = Cl or Br)

Complex (*z* = charge)	$E_{1/2}$/V[a]	
	$Ru^{IV/III}$	$Ru^{III/II}$
$[RuCl_4(CNXyl)_2]^{z}$[b]	+1.64 (qrev)[c,d]	−0.19 (qrev)[d,e]
$[RuBr_4(CNXyl)_2]^{z}$[b]	+1.48 (irrev)[c,d,f]	−0.08 (qrev)[d,e]
$[RuCl_4(CNBu^t)_2]^{z}$[b]	+1.53 (qrev)[c,d]	−0.28 (rev)[d,e]
$[RuBr_4(CNBu^t)_2]^{z}$[b]	+1.46 (irrev)[c,d,f]	−0.20 (rev)[d,e]
$[RuCl_3(CNXyl)_2(NCMe)]^{z}$[g]	—	+0.42 (rev)[h,i]
$[RuBr_3(CNXyl)_2(NCMe)]^{z}$[g]	—	+0.49 (rev)[h,i]

[a] *vs.* Ag–AgCl, against which ferrocenium–ferrocene is measured at +0.55 V, scan rate = 100 mV s^{-1}. In practice, $E°$ has been approximated by $E_{1/2}$, where $E_{1/2} = (E_{pa} + E_{pc})/2$, E_{pa} = anodic peak potential and E_{pc} = cathodic peak potential. rev = reversible, qrev = quasi-reversible, irrev = irreversible. [b] *trans* isomer. [c] *z* = 0/1− [d] Recorded in 0.5 mol dm^{-3} $[NBu_4][PF_6]$–CH_2Cl_2 at ≈213 K. [e] *z* = 1−/2− [f] Irreversible, E_{pa} quoted [g] *mer,trans* isomer. [h] Recorded in 0.1 mol dm^{-3} $[NBu_4][PF_6]$ in MeCN–CH_2Cl_2 (1 : 1) at ≈233 K. [i] *z* = 0/1−.

small yields of the desired complexes over extended reaction times (>2 weeks). Somewhat improved yields could be obtained by starting with an organo-soluble form of $[Ru_2Br_9]^{3-}$, but again the products were contaminated with bromide salts and repeated recrystallisation from a variety of solvents failed consistently to remove the impurities. It was found that the most convenient method to prepare pure samples of the complexes $[NBu_4][RuBr_4(CNR)_2]$ (R = Xyl or Bu^t) was that used for the analogous chloride complexes, *i.e.* the heating of $[NBu_4]_2[RuBr_6]$ in the presence of the chosen isocyanide ligand.

$[NBu_4][RuX_4(CNXyl)_2]$ (X = Cl or Br) was characterised by elemental analysis and a variety of spectroscopic techniques. Negative-ion FAB mass spectra gave molecular-ions corresponding to $[RuX_4(CNXyl)_2]^-$ and fragmentation patterns consistent with the sequential cleavage of halide and CNXyl (Table 1). Solutions of the complexes display UV-Vis spectra characteristic of *trans*-$[RuX_4L_2]^-$ species (where L is a neutral π-acceptor ligand).[4,13–17] The IR spectrum of each as a KBr disk contains a single strong band at 2150 (X = Cl) and 2148 cm^{-1} (X = Br) attributed to the ν_{NC} bands of the *trans* co-ordinated isocyanide ligands (ν_{NC} free ligand = 2123 cm^{-1}, KBr disc). The far-IR spectra are also consistent with the proposed stereochemistry, with bands having been located at 307 and 543 cm^{-1} (ν_{RuCl} and $\nu_{RuCNXyl}$) and 233 and 485 cm^{-1} (ν_{RuBr} and $\nu_{RuCNXyl}$).

General redox behaviour

The voltammetry of $[NBu_4][RuX_4(CNXyl)_2]$ (X = Cl or Br) is qualitatively similar to that of their $CNBu^t$ analogues,[1,2] *i.e.* both complexes display one-electron reduction and one-electron oxidation processes, as shown by coulometry. The data are summarised in Table 2, where the comparative data for $[NBu_4][RuX_4(CNBu^t)_2]$ are also presented. In accord with the anticipated differences between the electronic properties of the two isocyanide ligands, *i.e.* the net electron-donating ability of $CNBu^t$ is greater than that of CNXyl, the CNXyl complexes are reduced at a less negative potential than are their $CNBu^t$ analogues, whilst $[NBu_4][RuCl_4(CNXyl)_2]$ is oxidised at a more positive potential than $[NBu_4][RuCl_4(CNBu^t)_2]$. The oxidation of the analogous bromide complexes is irreversible in each case, even at low temperature, and consequently a comparison based on thermodynamic arguments is not strictly valid.

Electrochemical reduction of $[NBu_4][RuX_4(CNXyl)_2]$ in dichloromethane (X = Cl or Br)

The cyclic voltammograms of $[NBu_4][RuX_4(CNXyl)_2]$ and $[NBu_4][RuX_4(CNBu^t)_2]$ (X = Cl or Br) are shown in Figs. 1 and 2. The voltammetry in each case is recorded at room temperature in 0.5 mol dm^{-3} $[NBu_4][PF_6]$–dichloromethane in a glove-box under a nitrogen atmosphere. The major difference in the

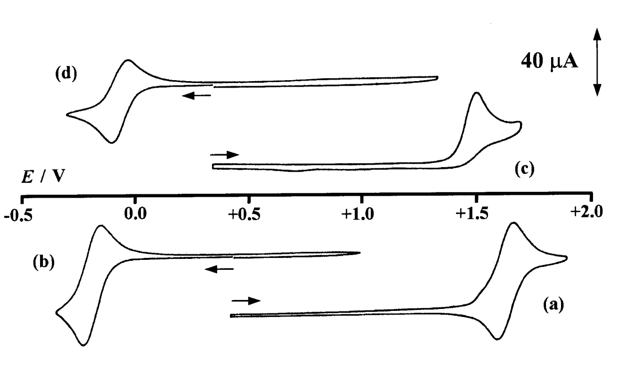

Fig. 1 (a), (b) Cyclic voltammograms of *trans*-$[NBu_4][RuCl_4(CNXyl)_2]$ in 0.5 mol dm^{-3} $[NBu_4][PF_6]$–dichloromethane at 293 K. (c), (d) Cyclic voltammograms of *trans*-$[NBu_4][RuBr_4(CNXyl)_2]$ in 0.5 mol dm^{-3} $[NBu_4][PF_6]$–dichloromethane at 293 K. Voltammetry recorded in a glove box. Scan rate = 100 mV s^{-1} in each case.

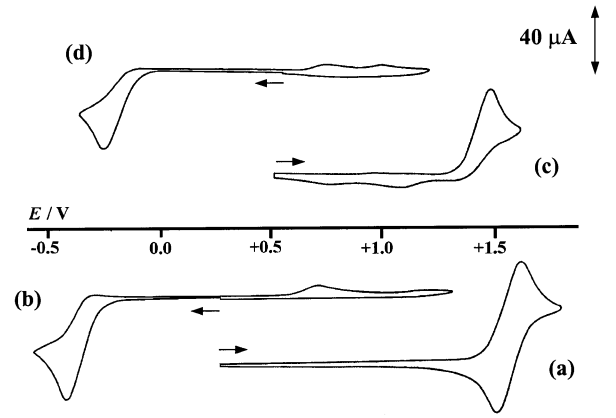

Fig. 2 (a), (b) Cyclic voltammograms of *trans*-$[NBu_4][RuCl_4(CNBu^t)_2]$ in 0.5 mol dm^{-3} $[NBu_4][PF_6]$–dichloromethane at 290 K. (c), (d) Cyclic voltammograms of *trans*-$[NBu_4][RuBr_4(CNBu^t)_2]$ in 0.5 mol dm^{-3} $[NBu_4][PF_6]$–dichloromethane at 293 K. Voltammetry recorded in a glove box. Scan rate = 100 mV s^{-1} in each case.

Table 3 IR data on *trans*-$[NBu_4][RuX_4(CNXyl)_2]$ and *mer,trans*-$[RuX_3(CNXyl)_2(NCMe)]$ (X = Cl or Br)

Complex (z = charge)	Band maxima/cm$^{-1\,a}$ ν_{NC}, Ru^{III}	ν_{NC}, Ru^{II}	ν_{CN}
$[RuCl_4(CNXyl)_2]^{z\,b\,c}$	2157 (s), $z = 1-$	2047 (m), 2004 (m), $z = 2-$	—
$[RuBr_4(CNXyl)_2]^{z\,b\,c}$	2150 (s), $z = 1-$	2043 (m), 2006 (m), $z = 2-$	—
$[RuCl_3(CNXyl)_2(NCMe)]^{z\,d\,e}$	2176 (s), $z = 0$	2076 (s), $z = 1-$	2328 (w) Ru^{III} 2274 (w) Ru^{II}
$[RuBr_3(CNXyl)_2(NCMe)]^{z\,d\,e}$	2171 (s), $z = 0$	2081 (s), $z = 1-$	2327 (w) Ru^{III} 2276 (w) Ru^{II}

[a] Recorded in an IRRAS cell under stated conditions. Relative band intensities; s = strong, m = medium and w = weak [b] *trans* isomer. [c] Recorded in 0.5 mol dm^{-3} $[NBu_4][PF_6]$–CH_2Cl_2 at ≈233 K. [d] *mer,trans* isomer. [e] Recorded in 0.1 mol dm^{-3} $[NBu_4][PF_6]$ in MeCN–CH_2Cl_2 (1 : 1) at ≈290 K.

voltammetry is that the Ru$^{III/II}$ reduction processes of $[NBu_4][RuX_4(CNXyl)_2]$ are quasi-reversible whereas those of the CNBu^t analogues are only partially reversible. The difference in reversibility is attributed to the capacity of the CNXyl ligand better to stabilise the reduced state through enhanced metal(dπ)-to-ligand(π*) back-bonding.

The reversibility of the *trans*-$[RuCl_4(CNXyl)_2]^{-/2-}$ couple on a voltammetric timescale offers the possibility of electrogenerating and characterising the dianion $[RuCl_4(CNXyl)_2]^{2-}$ *in situ*. The reduction of $[NBu_4][RuCl_4(CNXyl)_2]$ in 0.5 mol dm^{-3} $[NBu_4][PF_6]$–dichloromethane at 253 K was probed by IR spectroscopy, through performing the electrolysis in an IRRAS cell. Electroreduction at $E_{app} = -0.40$ V resulted in the collapse of the ν_{NC} band of the parent ion, $[RuCl_4(CNXyl)_2]^-$, at 2157 cm^{-1} (Table 3). Two bands grew simultaneously at lower wavenumber, a strong band at 2047 cm^{-1} and a weaker one at 2004 cm^{-1}. Re-oxidation at $E_{app} = 0.00$ V led to quantitative reformation of the original $[RuCl_4(CNXyl)_2]^-$ spectrum. These spectral changes are consistent with the chemically reversible process summarised in eqn. (1).

The IR spectrum of $[RuCl_4(CNXyl)_2]^-$, in which the CNXyl ligand co-ordinates to Ru^{III} through a pure σ-bond interaction, ‡ [18] displays only one ν_{NC} band and therefore the ion must approximate to D_{4h} symmetry. However upon reduction the symmetry is thought to be lowered through bending along the Ru–CN–C axis, as the π* orbital of the isocyanide ligand is populated by back-bonding from the Ru^{II} centre. This lowering in symmetry leads to the observation of two ν_{NC} bands from the co-ordinated isocyanide ligands.[19,20]

Two ν_{NC} bands in the IR spectrum of the reduced species could also arise if isomerisation to *cis*-$[RuCl_4(CNXyl)_2]^{2-}$ were to occur; however this possibility is discounted on the basis of the appearance of the cyclic voltammogram and the potentials at which re-oxidation occurs in the spectroelectrochemical experiments. The potential of the Ru$^{III/II}$ process is anticipated to be significantly different for the *cis* and *trans* isomers of $[RuCl_4(CNXyl)_2]^-$. For the related osmium complexes, the Os$^{III/II}$ reduction potentials (z = 1−/2−) of the *cis* and *trans* isomers of $[OsCl_4L_2]^z$ can differ considerably, from 0.18 V for L = py to 0.82 V for L = CO.[21,22] However, the appearance of the voltammogram of *trans*-$[RuCl_4(CNXyl)_2]^-$ under a variety of conditions (scan rate and temperature) remains essentially unchanged, in that the return wave (E_{pa}) remains *ca.* 80 mV from the forward wave (E_{pc}).

If the isomerisation were slow on the timescale of the cyclic voltammogram, a reversible wave might still be observed. However under these circumstances re-oxidation in the spectroelectrochemical experiment which, relative to the cyclic voltammetric experiment, has a longer time domain, would not have occurred at such a negative potential, *i.e.* the re-oxidation of $[RuCl_4(CNXyl)_2]^{2-}$ at $E_{app} = 0.00$ V, which led to the quantitative reformation of *trans*-$[RuCl_4(CNXyl)_2]^-$, is not consistent with *trans–cis* isomerisation following reduction.

The reduction of $[NBu_4][RuCl_4(CNXyl)_2]$ was also probed by UV-Vis spectroelectrochemistry and was found to be reversible on the timescale of the OTTLE experiment. The UV-Vis spectrum of the parent-ion, *trans*-$[RuCl_4(CNXyl)_2]^-$, is shown in Fig. 3(a). The spectrum shows the characteristic signature of the planar four-halide chromophore, and is similar to that of other *trans*-$[MX_4L_2]^z$ complexes where M is a low-spin metal ion with a d^5 electron configuration.[4,13–17] The weak leading band at 503 nm is assigned to the spin-forbidden a_{2g}(Cl pπ) to b_{2g}(Ru dπ) ligand-to-metal charge-transfer transition,[13] whilst the intense band at 430 nm is assigned to the related e_u(Cl pπ) to b_{2g}(Ru dπ) transition.[13,14] Upon low temperature (233 K) reduction at $E_{app} = -0.40$ V these bands collapse and an intense band grows at 365 nm (Fig. 3b). This latter band, and the shoulder at 339 nm, are assigned to metal-to-ligand charge-transfer transitions, e_g(Ru dπ) to e_u(CNXyl π*).[13] The spectral changes accompanying reduction occur with the retention of isosbestic points, and re-oxidation at $E_{app} = 0.00$ V results in the quantitative reformation of the starting spectrum. The low temperature reduction of the analogous bromide complex, $[NBu_4][RuBr_4(CNXyl)_2]$, is also chemically reversible on the timescale of the OTTLE experiment. The important features of the relevant spectra are listed in Table 4.

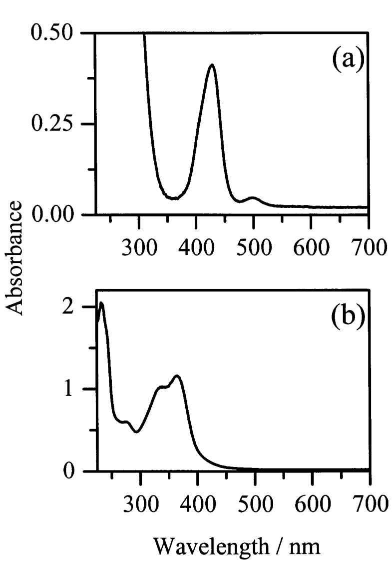

Fig. 3 UV-Vis spectra of (a) *trans*-$[RuCl_4(CNXyl)_2]^-$ and (b) *trans*-$[RuCl_4(CNXyl)_2]^{2-}$, recorded in acetonitrile–dichloromethane (1 : 1, v : v) containing 0.25 mol dm^{-3} $[NBu_4][PF_6]$ at 233 K in an OTTLE cell.

Electrochemical reduction of $[NBu_4][RuX_4(CNXyl)_2]$ in acetonitrile (X = Cl or Br)

The reduction of $[NBu_4][RuX_4(CNXyl)_2]$ (X = Cl or Br) can also lead to the formation of substituted species where halide is

---

‡ ν_{NC} for the free ligand (CNXyl) occurs at 2123 cm^{-1}, when measured in dichloromethane containing 0.5 mol dm^{-3} $[NBu_4][PF_6]$. ν_{NC} for $[NBu_4][RuCl_4(CNXyl)_2]$ under identical conditions occurs at 2157 cm^{-1}; thus ν_{NC} (complex) > ν_{NC} (free ligand).

Table 4 UV-Vis data on *trans*-$[NBu_4][RuX_4(CNXyl)_2]$ and *mer*,*trans*-$[RuX_3(CNXyl)_2(NCMe)]$ (X = Cl or Br)

Complex (z = charge)	Band maxima/nm (ε/dm^3 mol^{-1} cm^{-1})[a] Ru^{III}	Ru^{II}
$[RuCl_4(CNXyl)_2]^{z}$ [b,c]	503 (300)	365 (10500)
	430 (3700)	≈339 sh (≈9000)
	276 (30000)	272 (5400)
	236 (42000)	
$[RuBr_4(CNXyl)_2]^{z}$ [b,e]	694 w	366 (27000)
	588 (10000)	≈341 sh (≈24000)
	545 (7100)	279 (27000)
	495 (2100)	
	458 (3300)	
	281 (28000)	
$[RuCl_3(CNXyl)_2(NCMe)]^{z}$ [d,f]	500 (850)	328 (11000)
	427 (3200)	
$[RuBr_3(CNXyl)_2(NCMe)]^{z}$ [d,f]	690 (700)	347 sh (≈9000)
	584 (3100)	319 (13000)

[a] Recorded in an OTTLE cell under stated conditions. [b] *trans* isomer. [c] Recorded in 0.25 mol dm^{-3} $[NBu_4][PF_6]$ in MeCN–CH_2Cl_2 (1 : 1) at ≈233 K. [d] *mer*,*trans* isomer. [e] Recorded in 0.5 mol dm^{-3} $[NBu_4][PF_6]$ in CH_2Cl_2 at ≈353 K. [f] Recorded in 0.25 mol dm^{-3} $[NBu_4][PF_6]$ in MeCN–CH_2Cl_2 (1 : 1) at ≈293 K.

replaced by another ligand which better stabilises the reduced state. For example, reduction of *trans*-$[RuX_4(CNXyl)_2]^-$ in the presence of acetonitrile results in the formation of *mer*,*trans*-$[RuX_3(CNXyl)_2(NCMe)]^-$, which can be oxidised reversibly to *mer*,*trans*-$[RuX_3(CNXyl)_2(NCMe)]$. The complexes *trans*-$[NBu_4][RuX_4(CNBu^t_2)]$ (X = Cl or Br) form analogous mono-substituted species in the presence of acetonitrile.[1] The cyclic voltammogram of $[NBu_4][RuCl_4(CNXyl)_2]$ recorded in dichloromethane–acetonitrile (1 : 1, v : v) containing 0.25 mol dm^{-3} $[NBu_4][PF_6]$ at 293 K is shown in Fig. 4. A partially-reversible reduction is detected at E_{pc} −0.31 V. On the return scan two additional waves are detected that are not present if the forward scan is reversed prior to the reduction at E_{pc} −0.31 V (Fig. 4a). These waves, at E_{pa} = +0.38 and +1.17 V, are attributed to oxidation of the mono-substituted species *mer*,*trans*-$[RuCl_3(CNXyl)_2(NCMe)]^-$ and chloride respectively. Switching the return scan at approximately +0.60 V (Fig. 4b) shows that re-reduction of *mer*,*trans*-$[RuCl_3(CNXyl)_2(NCMe)]$ is chemically reversible on the timescale of the voltammetric experiment. The series of events leading to the formation are summarised in eqn. (1)–(3).

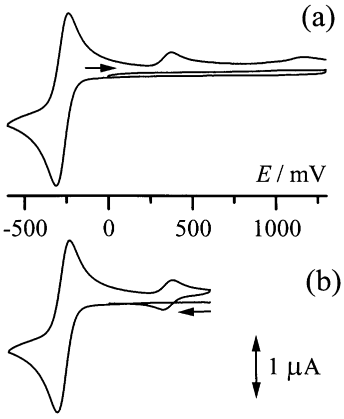

Fig. 4 (a), (b) Cyclic voltammograms of *trans*-$[NBu_4][RuCl_4(CNXyl)_2]$ in an acetonitrile solution containing 0.25 mol dm^{-3} $[NBu_4][PF_6]$ at 293 K. Scan rate = 100 mV s^{-1} in each case.

$$\textit{trans}\text{-}[RuX_4(CNR)_2]^- + e^- \overset{E_1^o,\,k_{s1}}{\rightleftharpoons} \textit{trans}\text{-}[RuX_4(CNR)_2]^{2-} \quad (1)$$

$$\textit{trans}\text{-}[RuX_4(CNR)_2]^{2-} + MeCN \xrightarrow{k} \textit{mer,trans}\text{-}[RuX_3(CNR)_2(NCMe)]^- + X^- \quad (2)$$

$$\textit{mer,trans}\text{-}[RuX_3(CNR)_2(NCMe)]^- \overset{E_2^o,\,k_{s2}}{\rightleftharpoons} \textit{mer,trans}\text{-}[RuX_3(CNR)_2(NCMe)] + e^- \quad (3)$$

The reductive elimination of halide and subsequent co-ordination of acetonitrile can be conveniently monitored by IR spectroscopy upon performing the reduction in an IRRAS cell. The IR spectral changes which accompany the reduction of $[NBu_4][RuCl_4(CNXyl)_2]$ in 0.10 mol dm^{-3} $[NBu_4][PF_6]$ in acetonitrile : dichloromethane (1 : 1, v : v) at 293 K are shown in Fig. 5. Upon reduction at E_{app} = −0.50 V, the ν_{NC} band of the parent ion collapses, as shown in the difference spectrum by the growth in negative absorbance at 2154 cm^{-1} (Fig. 5a). The formation of the transient species *trans*-$[RuCl_4(CNXyl)_2]^{2-}$ is shown by the growth of bands at 2039 and 2001 cm^{-1} (note that the positions of these bands are somewhat solvent dependent). These bands subsequently collapse as *trans*-$[RuCl_4(CNXyl)_2]^{2-}$ is converted to *mer*,*trans*-$[RuCl_3(CNXyl)_2(NCMe)]^-$, which has a single ν_{NC} band at 2076 cm^{-1}. The latter ion can be oxidised reversibly to *mer*,*trans*-$[RuCl_3(CNXyl)_2(NCMe)]$ at E_{app} = +0.50 V, whereupon the ν_{NC} band at 2076 cm^{-1} collapses and another grows at 2176 cm^{-1} (Fig. 5b), in addition to a very weak band at 2328 cm^{-1} from co-ordinated acetonitrile. The analogous bromide complex behaves similarly (Table 3).

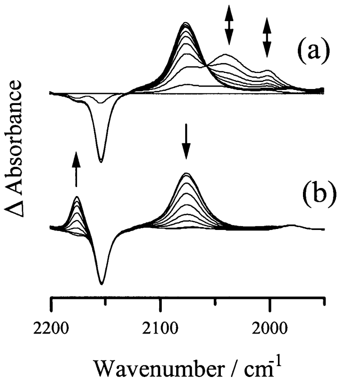

Fig. 5 (a) Changes in the IR difference absorption spectra accompanying reduction of *trans*-$[NBu_4][RuCl_4(CNXyl)_2]$ in 0.10 mol dm^{-3} $[NBu_4][PF_6]$ in acetonitrile–dichloromethane (1 : 1, v : v) in an IRRAS cell at 293 K. The horizontal line at zero absorbance corresponds to the initial spectrum, *i.e.* that of *trans*-$[RuCl_4(CNXyl)_2]^-$, prior to electrolysis, ratioed against itself. The potential of the working electrode is stepped to E_{app} = −0.50 V, and single scan IR spectra are collected as a function of time (2 s interval). Consumption of *trans*-$[RuCl_4(CNXyl)_2]^-$ upon reduction, is indicated by increasing negative absorbance at 2154 cm^{-1}. (b) Re-oxidation is achieved at E_{app} = +0.50 V, whereupon the band at 2076 cm^{-1} collapses and another grows at 2176 cm^{-1}.

The conversion of *trans*-$[NBu_4][RuX_4(CNXyl)_2]$ to *mer*,*trans*-$[RuX_3(CNXyl)_2(NCMe)]^-$ and the subsequent oxidation of this latter species can also be followed by UV-Vis spectroscopy by performing the electrolyses in an OTTLE cell (Table 4).

Kinetics of substitution of halide by acetonitrile upon electrochemical reduction of $[NBu_4][RuX_4(CNR)_2]$ (X = Cl or Br, R = Bu^t or Xyl)

Some ligand dependent differences in the rate of substitution of the $[RuX_4(CNR)_2]^{2-}$ ions were apparent from voltammetric and spectroelectrochemical studies. In order to quantify the difference in substitution kinetics, the voltammetry of $[NBu_4][RuX_4(CNXyl)_2]$ and $[NBu_4][RuX_4(CNBu^t)_2]$ (X = Cl or Br) was simulated using DigiSim®. The mechanism proposed to account for the formation of the mono-substituted species and

Table 5 Kinetic data obtained for $[NBu_4][RuBr_4(CNBu^t)_2]$ in 1 : 1, 3 : 1 and 1 : 0 acetonitrile–dichloromethane mixtures obtained by simulation of cyclic voltammograms at scan rates over the range 100 to 1000 mV s^{-1}

MeCN : CH_2Cl_2 ratio	D^a/cm^2 s^{-1}	$\Delta E^{\circ b}$/V	$k_{s1}{}^c$/cm s^{-1}	$k_{s2}{}^c$/cm s^{-1}	k'^{d}/s^{-1}	[MeCN]^e/mol dm^{-3}	k^f/mol^{-1} dm^{-3} s^{-1}
1 : 1	8.0×10^{-6}	0.606	0.020	0.030	2.750	9.57	0.287
3 : 1	1.1×10^{-5}	0.606	0.030	0.050	4.125	14.36	0.287
1 : 0	1.1×10^{-5}	0.606	0.050	0.065	5.500	19.15	0.287

[a] D = diffusion coefficient. [b] $\Delta E^\circ = E_2^\circ - E_1^\circ$. [c] k_{s1}, k_{s2} = heterogeneous charge transfer rate constant. [d] k' = pseudo first-order rate constant. [e] Concentration of acetonitrile. [f] k = second-order rate constant.

Table 6 Kinetic data obtained for $[NBu_4][RuX_4(CNR)_2]$ (X = Cl or Br, R = Bu^{t}or Xyl) in 1 : 1 acetonitrile–dichloromethane obtained by simulation of cyclic voltammograms at scan rates over the range 100 to 1000 mV s^{-1}

Complex	D^a/cm^2 s^{-1}	$\Delta E^{\circ b}$/V	$k_{s1}{}^c$/cm s^{-1}	$k_{s2}{}^c$/cm s^{-1}	k'^{d}/s^{-1}	k^e/mol^{-1} dm^3 s^{-1}
$[NBu_4][RuBr_4(CNBu^t)_2]$	8.0×10^{-6}	0.606	0.020	0.030	2.750	0.287
$[NBu_4][RuCl_4(CNBu^t)_2]$	8.5×10^{-6}	0.664	0.090	0.200	2.200	0.230
$[NBu_4][RuBr_4(CNXyl)_2]$	1.0×10^{-5}	0.571	0.040	0.200	0.100	0.0104
$[NBu_4][RuCl_4(CNXyl)_2]$	7.8×10^{-6}	0.620	0.030	0.090	0.090	0.00936

[a] D = diffusion coefficient. [b] $\Delta E^\circ = E_2^\circ - E_1^\circ$. [c] k_{s1}, k_{s2} = heterogeneous charge transfer rate constant. [d] k' = pseudo first-order rate constant. [e] k = second-order rate constant.

its subsequent oxidation is summarised in eqn. (1)–(3), where E_1° and E_2° are the reversible formal potentials for processes 1 and 3 respectively, k_{s1} and k_{s2} are the heterogeneous charge-transfer rate constants and the charge-transfer coefficients are assumed to be 0.5.

Eqn. (2) may be explained in terms of a second-order rate law as given in eqn. (4), where v is the rate and k is the second-order rate constant. In all experiments the concentration of acetonitrile is in large excess and may be assumed to be constant. The effective rate law becomes pseudo first-order [eqn. (5)], where k' is the pseudo first-order rate constant. The value of k' obtained from the simulation may be converted to k using eqn. (6) and the concentration of acetonitrile.

$$v = k\{[RuX_4(CNR)_2]^{2-}\}\{[NCMe]\} \qquad (4)$$

$$v = k'\{[RuX_4(CNR)_2]^{2-}\} \qquad (5)$$

$$k' = k[MeCN] \qquad (6)$$

Voltammograms were recorded in 1 : 1 mixtures of acetonitrile and dichloromethane at a number of different scan rates (100, 200, 500 and 1000 mV s^{-1}). In order to verify the proposed second-order mechanism, additional voltammograms for $[NBu_4][RuBr_4(CNBu^t)_2]$ were recorded in 3 : 1 and 1 : 0 acetonitrile–dichloromethane mixtures. For these experiments solutions containing 0.5–1.0 mmol dm^{-3} of complex and 0.1 mol dm^{-3} $[NBu_4][PF_6]$ of electrolyte were used. In the simulations, the diffusion coefficients of the redox products were assumed to be the same as those of the starting complex. Experiments were performed and simulated at 293 K, a 0.0275 cm^2 platinum macrodisc electrode was used and the uncompensated resistances were taken to be between 200 and 300 Ω depending on the solvent mixture. Although capacitances are incorporated into the simulations, it is not possible to take into account the potential dependence of the background current, which explains the differences between the simulation and experimental data. Step 2 [eqn. (2)] was assumed to be completely irreversible. Thus, solely for the purposes of the simulation, a high (1000) but chemically insignificant value for the equilibrium constant was used.

The simulation and experimental details are listed in Tables 5 and 6, and Fig. 6 shows an example of the experimental and simulation outcome. The second-order rate constant k was found to increase in the order X = Cl, R = Xyl < X = Br, R = Xyl < X = Cl, R = Bu^t < X = Br, R = Bu^t. The order is consistent with qualitative observations, *viz.* rate of substitution of Br > Cl and CNBu^t > CNXyl.

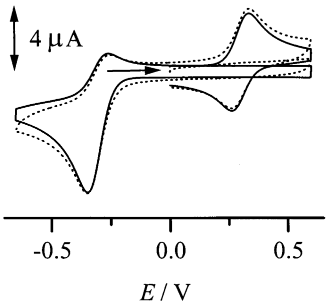

Fig. 6 Experimental (–) and simulated (- - -) cyclic voltammograms of *trans*-$[NBu_4][RuBr_4(CNBu^t)_2]$ in 0.1 mol dm^{-3} $[NBu_4][PF_6]$ acetonitrile–dichloromethane (1 : 1, v : v) at 500 mV s^{-1} (293 K).

Electrochemical oxidation of $[NBu_4][RuX_4(CNXyl)_2]$ (X = Cl or Br)

The cyclic voltammogram of $[NBu_4][RuCl_4(CNXyl)_2]$, when recorded in dichloromethane, reveals a small pre-wave at the foot of the $[RuCl_4(CNXyl)_2]^{-/0}$ process. Attempts to electrogenerate *trans*-$[RuCl_4(CNXyl)_2]$ quantitatively in either the IRRAS or OTTLE cells failed due to passivation of the electrode. The pre-wave is absent when the voltammetry is recorded in acetonitrile, and the oxidation remains chemically reversible on the time-scale of the voltammetric experiment. However, despite the improvement in the voltammetry, the oxidation of $[RuCl_4(CNXyl)_2]^-$ was shown to be chemically irreversible on the timescales of the IR and UV-Vis spectroelectrochemical experiments, even at low temperature. The spectral changes that accompanied electrolysis indicated the formation of multiple species, which was confirmed by the observation of four processes in the cyclic voltammogram of a solution of $[NBu_4][RuCl_4(CNXyl)_2]$ following bulk electrolysis at $E_{app} = +1.70$ V (Fig. 7). Of those species formed, only *mer*,*trans*-$[RuCl_3(CNXyl)_2(NCMe)]$ ($E_{1/2} = +0.42$ V) and *trans*,*trans*,*trans*-$[RuCl_2(CNXyl)_2(NCMe)_2]^+$ ($E_{1/2} = +1.04$ V) were identified conclusively by cyclic voltammetry and IR spectroscopy.[23,24] The species which give rise to the processes at $E_{1/2} = +0.77$ V and $E_{1/2} = +1.22$ V in Fig. 7 remain unidentified.

The cyclic voltammetry of $[NBu_4][RuBr_4(CNXyl)_2]$ reveals an irreversible oxidation in either dichloromethane or acetonitrile, even at the low temperature limits of these solvents.

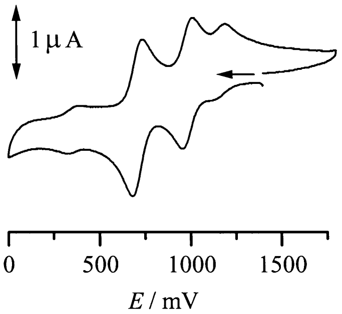

Fig. 7 Cyclic voltammogram of *trans*-$[NBu_4][RuCl_4(CNXyl)_2]$ in an acetonitrile solution containing 0.25 mol dm^{-3} $[NBu_4][PF_6]$ at 293 K after bulk electrolysis at $E_{app} = +1.70$ V. Scan rate = 100 mV s^{-1}.

Unlike its chloride analogue, however, there is only one product formed upon oxidation in the presence of acetonitrile. Oxidation results in the quantitative formation of *mer*,*trans*-$[RuBr_3(CNXyl)_2(NCMe)]$, as shown by IR and UV-Vis spectroelectrochemistry (Tables 3 and 4). This is an unusual example of oxidative and reductive activation yielding complexes of identical stoichiometry and geometry, albeit that they are not isoelectronic.

The ultimate formation of various substituted tervalent products from oxidation of $[RuX_4(CNXyl)_2]^-$ (X = Cl or Br) is thought to occur *via* oxidatively induced reductive elimination of halide.[1] Despite the tendency of halides to stabilise higher oxidation states,[13] in certain circumstances cleavage of a metal–halide bond(s) has been shown to take place upon oxidation.[25,26] The mechanism is believed to involve metal-based oxidation followed by homolytic fission of M–X bond(s). In this particular case, oxidation to Ru^{IV}-X would be followed by homolytic fission to yield Ru^{III} (with a vacant co-ordination site) and $X^\bullet$. For the analogous $CNBu^t$ complexes, the tetravalent complex $[RuCl_4(CNBu^t)_2]$ was stable at low temperature and characterised *in situ* (IR and UV-Vis). At ambient temperature however, $[RuCl_4(CNBu^t)_2]$ was short-lived and decomposed to a variety of tervalent species.[2] For the bromide complex $[NBu_4][RuBr_4(CNBu^t)_2]$, only one product, *mer*,*trans*-$[RuBr_3(CNBu^t)_2(NCMe)]$, is obtained upon oxidation. *In situ* EPR studies of $[NBu_4][RuBr_4(CNBu^t)_2]$ in the presence of a spin-trap revealed the formation of radical species upon oxidation, however they were not identified conclusively.[27]

Conclusions

The chemical synthesis and characterisation of two previously unreported complexes, *trans*-$[NBu_4][RuX_4(CNXyl)_2]$ (X = Cl or Br), have been described and their redox chemistry investigated using electrochemical and spectroelectrochemical techniques. The redox behaviour of these complexes is in general similar to that of the related complexes *trans*-$[NBu_4][RuX_4(CNBu^t)_2]$, in that each displays a one-electron reduction and oxidation. The one-electron reduced species, *trans*-$[RuX_4(CNXyl)_2]^{2-}$, have been electrogenerated *in situ* and characterised by both IR and UV-Vis spectroscopy. The analogous $CNBu^t$ species had previously been found to be insufficiently stable for characterisation; the CNXyl ligand is better able to stabilise the reduced state on account of its π* orbital being relatively lower in energy than that for $CNBu^t$. The reduction of *trans*-$[NBu_4][RuX_4(CNXyl)_2]$ (X = Cl or Br) in the presence of acetonitrile produces the mono-substituted species, *mer*,*trans*-$[RuX_3(CNXyl)_2(NCMe)]^-$, which can be oxidised reversibly to *mer*,*trans*-$[RuX_3(CNXyl)_2(NCMe)]$. The voltammetry associated with this redox-activated ligand exchange reaction has been simulated to provide an estimate for the rate constant of each substitution reaction; these were found to vary in the order X = Cl, R = Xyl < X = Br, R = Xyl < X = Cl, R = Bu^t < X = Br, R = Bu^t. Like its $CNBu^t$ analogue, oxidation of *trans*-$[NBu_4][RuCl_4(CNXyl)_2]$ in the presence of acetonitrile yields several tervalent products *via* oxidatively induced reductive elimination of $X^\bullet$. In comparison, oxidation of *trans*-$[NBu_4][RuBr_4(CNXyl)_2]$ under identical conditions produces only *mer*,*trans*-$[RuBr_3(CNXyl)_2(NCMe)]$.

Acknowledgements

The authors thank Johnson Matthey p.l.c. for the loan of hydrated ruthenium trichloride and the Central Research Fund of the University of London for financial assistance. D. G. H. acknowledges the Royal Society and the Australian Research Council for an Endeavour Fellowship and the Ramsay Memorial Fellowships Trust for a British Ramsay Memorial Fellowship. J. P. A. thanks the EPSRC for a postgraduate award. N. C. H. acknowledges the Royal Society for an Australian Research Fellowship.

References

1 J. P. al Dulaimi, R. J. H. Clark and D. G. Humphrey, *J. Chem. Soc., Dalton Trans.*, 1997, 2535.
2 J. P. al Dulaimi, R. J. H. Clark and D. G. Humphrey, *J. Chem. Soc., Dalton Trans.*, 2000, 933.
3 F.-W. Lee, M.-Y. Choi, K.-K. Cheung and C.-M. Che, *J. Organomet. Chem.*, 2000, **595**, 114.
4 C. M. Duff and R. A. Schmid, *Inorg. Chem.*, 1991, **30**, 2938.
5 J. P. al Dulaimi, R. J. H. Clark, M. Saavedra S. and Md. A. Salam, *Inorg. Chim. Acta*, 2000, **300–302**, 525.
6 W. P. Griffith, *J. Chem. Soc., Dalton Trans.*, 1985, 1673.
7 W. Preetz and H. N. v. Allwörden, *Z. Naturforsch., Teil B*, 1987, **42**, 381.
8 R. J. H. Clark and D. G. Humphrey, *Inorg. Chem.*, 1996, **35**, 2053.
9 A. M. Bond, Kh. Z. Brainina and M. Koppenol, *Electroanalysis*, 1994, **6**, 275.
10 M. Rudolph, D. P. Reddy and S. W. Feldberg, *Anal. Chem.*, 1994, **66**, 589A.
11 S. P. Best, S. A. Ciniawsky and D. G. Humphrey, *J. Chem. Soc., Dalton Trans.*, 1996, 2945.
12 S. P. Best, R. J. H. Clark, R. P. Cooney and R. C. S. McQueen, *Rev. Sci. Instrum.*, 1987, **58**, 2071.
13 C. M. Duff and G. A. Heath, *J. Chem. Soc., Dalton Trans.*, 1991, 2401.
14 I. M. Bell, R. J. H. Clark and D. G. Humphrey, *J. Chem. Soc., Dalton Trans.*, 1999, 1307.
15 D. L. Key, L. F. Larkworthy and J. E. Salmon, *J. Chem. Soc. A*, 1971, 2583.
16 E. Alessio, G. Balducci, M. Calligaris, G. Costa, W. Attia and G. Mestroni, *Inorg. Chem.*, 1991, **30**, 609.
17 E. Alessio, M. Bolle, B. Milani, G. Mestroni, P. Faleschini, S. Geremia and M. Calligaris, *Inorg. Chem.*, 1991, **30**, 609.
18 J. A. Connor, E. M. Jones, G. K. McEwen, M. K. Lloyd and J. A. McCleverty, *J. Chem. Soc., Dalton Trans.*, 1972, 1246.
19 L. Verdonck, T. Tulunt and G. P. Van der Kelen, *Spectrochim. Acta*, 1979, **35A**, 867.
20 C. J. Cameron, R. A. Walton and D. A. Edwards, *J. Organomet. Chem.*, 1984, **262**, 335.
21 G. A. Heath, D. G. Humphrey and D. Menglet, unpublished work.
22 K. J. Taylor and L. J. Yellowlees, *Abstracts from 4th International Conference on the Chemistry of the Platinum Group Metals*, July 1990, C-36.
23 J. P. al Dulaimi, R. J. H. Clark, M. Saavedra S. and Md. A. Salam, *Inorg. Chim. Acta*, 2000, **300–302**, 175.
24 D. G. Humphrey and A. M. Bond, unpublished work.
25 J. C. Kotz, W. Vining, W. Coco and R. Rosen, *Organometallics*, 1983, **2**, 68.
26 D. R. Tyler, *Prog. Inorg. Chem.*, 1988, **36**, 125.
27 D. G. Humphrey, A. M. Bond and G. Lazarev, unpublished work.